



# Domain Wall Trapping and Influence of the Asymmetry in Magnetic Nanoring Studied by Micromagnetic Simulations

X. H. Wang, W. Z. Wang, T. F. Kong, and W. S. Lew\*

*Physics and Applied Physics Division, School of Physical and Mathematical Sciences,  
Nanyang Technological University, 21 Nanyang Link, Singapore 637371*

We have studied the magnetic switching behavior of permalloy asymmetric rings using micromagnetic simulations. The simulation results have revealed that a domain wall trapping feature is present at the narrow arm of the asymmetric ring. This trapping feature is obtained via precise control of the lateral geometric features, the ring asymmetry and the film thickness. Our results show that the trapped domain walls do not annihilate until the magnetization in the wide arm is reversed under a relatively large magnetic field. Furthermore, the magnetic field strength needed to annihilate the domain wall is found to be decreasing with larger asymmetry ratio.

**Keywords:** Domain Wall Trapping, Asymmetric, Magnetic Nanoring.

## 1. INTRODUCTIONS

Geometrically confined domain walls in small magnetic elements have been extensively studied for years because of their potential applications in data storage,<sup>1</sup> magnetic logic<sup>2</sup> and sensing devices.<sup>3</sup> With the advent of modern nanofabrication and characterization techniques, we are able to engineer and observe new magnetism in the magnetic elements on the nanoscale. In order to make use of domain wall in a memory device, it is imperative to understand the domain wall position, and control it electrically and magnetically for optimum performance. There are efforts to study domain walls behavior in nanowires or nanoscale ring structures that contain specific geometrical features. For instance, by introducing notches<sup>4</sup> or protrusions<sup>5</sup> into nanowires or nanorings, attractive potential wells have been formed, with that, the domain walls can be trapped effectively at a designated position. Manipulating the trapped domain wall has potential applications in magnetic logic devices.<sup>6</sup> Other possible application of trapped domain wall is the use of a localized domain wall oscillator as a tunable microwave source.<sup>7</sup> In this work, we have used micromagnetic simulation to study nanoscale asymmetric ring structure that has an off-centered inner circle. Our results show that by controlling the dimensions of the asymmetric rings, a local vortex core free switching process can be obtained, and a pair of head-to-head and

tail-to-tail domain wall is trapped at the narrow arm of the asymmetric ring. We have also observed that when the asymmetry ratio of the ring increases, the magnetic field needed to annihilate the trapped domain walls becomes smaller.

## 2. SIMULATIONS

The magnetization configuration and switching processes were simulated using the OOMMF simulation program.<sup>8</sup> Figure 1 shows the geometry of the asymmetric ring used in the simulation. We define an asymmetry ratio  $R$  as the distance between the centers of the two circles  $l$  to the difference between the outer diameter  $D_o$  and the inner diameter  $D_i$ , i.e.,  $R = l / (D_o - D_i)$ . In the simulation, we choose permalloy asymmetric ring that has a lateral dimension of  $D_o = 600$  nm and  $D_i = 300$  nm to investigate the influence of the film thickness and the ring asymmetry on the switching behaviors. A range of film thickness, from 8 nm to 16 nm was used, and ring asymmetry ratios of 0.1, 0.2 and 0.3 were selected. The micromagnetic equilibrium equation was solved in the 2D simulations using a two dimensional square mesh with a cell size of 4 nm. The simulation parameters used for the permalloy thin film were: magnetic anisotropy constant  $K_1 = 0$ , saturation magnetization  $M_s = 8.6 \times 10^5$  Am<sup>-1</sup>, exchange constant  $A = 1.3 \times 10^{-11}$  Jm<sup>-1</sup> and damping coefficient  $\alpha = 0.4$ . A ramping magnetic field of  $-2000$  Oe to  $2000$  Oe in 200 steps was applied.

\* Author to whom correspondence should be addressed.

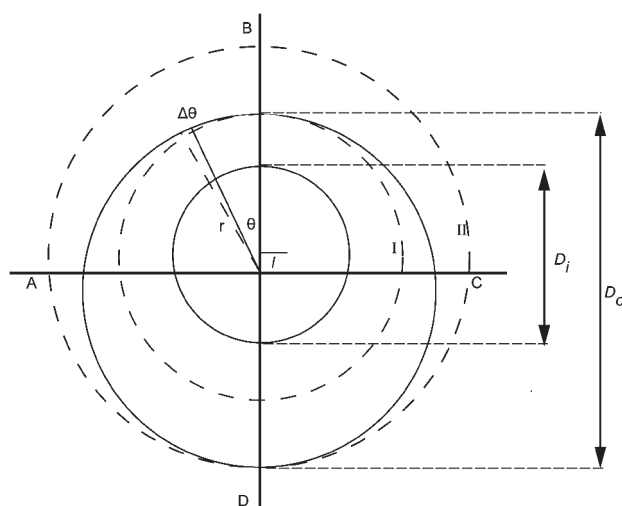


**Fig. 1.** The geometry of the model used in the simulations. An asymmetric ring ratio of  $R = 0.2$  is shown here.

### 3. RESULTS AND DISCUSSION

Figure 2(a) shows a typical simulated hysteresis loop of the asymmetric ring with a thickness of 16 nm and an asymmetry ratio of  $R = 0.2$ . Insets show the corresponding magnetic configurations with different magnetic field strengths applied: negative saturation, bi-domain, vortex, reverse bi-domain, and positive saturation. The double switch shown in the hysteresis loop is due to the propagation of the domain walls via both the narrow and the wide arms of the asymmetric ring. Figure 2(b) shows the simulated hysteresis loop of an 8-nm-thick asymmetric ring which has four switches. The first switch happens at the relatively low field of  $-5$  mT is caused by the domain wall movement via the narrow arm of the asymmetric ring. The second and third switches at the magnetic field around  $30\sim 40$  mT are caused by the domain wall movement via the wide arm of the asymmetric ring and then annihilation. The domain wall trapping behavior in the 8-nm-thick asymmetric ring happens between the first two switches of the reversal process: instead of forming a flux-closure state after the bi-domain state, the two domain walls at the narrow arm of the ring do not annihilate, but traps a pair of head-to-head and tail-to-tail domain walls, as shown in the insets of Figure 2(b). The trapped domain walls are stable until the annihilation of the domain walls in the wide arm of the asymmetric ring when a relatively large magnetic field is applied. This annihilation of the domain walls trapped at the narrow arm explains the existence of the switch before reaching saturation in the hysteresis loop of the 8-nm-thick asymmetric ring.

The domain wall trapping behavior occurring in the narrow arm of the asymmetric ring is possibly due to the significant increase in the exchange energy, as a result of

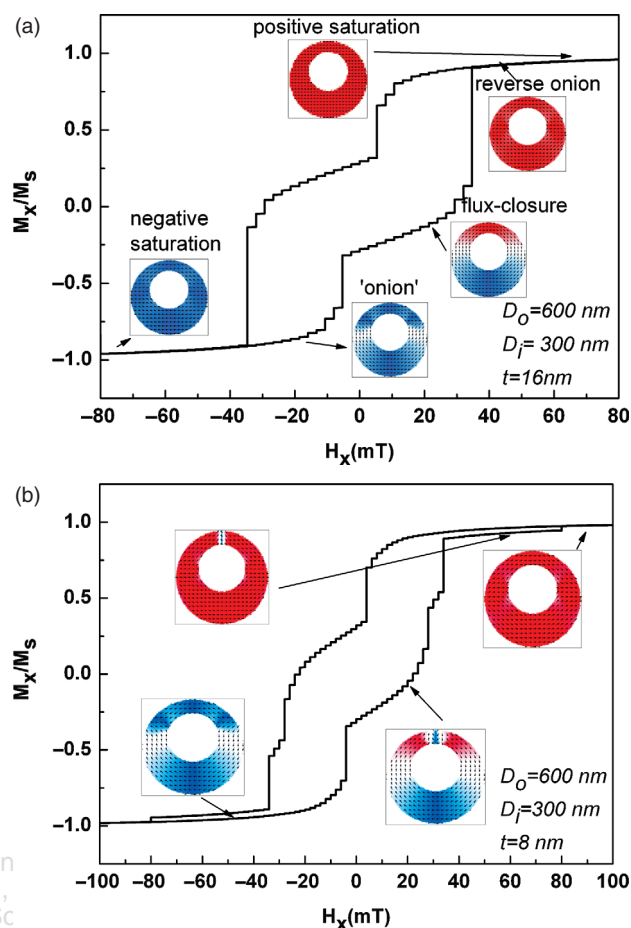


**Fig. 2.** Typical simulated hysteresis loops for (a) 16-nm-thick, (b) 8-nm-thick asymmetric magnetic rings. The outer diameter  $D_o$  is 600 nm. Insets show the spin configurations at different field strength.

the film thickness approaching the exchange length of the material. The increase in the exchange energy complicates the formation of a flux-closure state in the asymmetric ring. We have also used different  $l$  values to study the influence of the ring asymmetry on the switching process. It is found that the ring asymmetry plays a less important role in the domain wall trapping; that is, for asymmetric ring with similar thickness, the change of the ring asymmetry ratio  $R$  does not affect the presence of the domain wall trapping behavior. The only difference is that the annihilation of the trapped domain walls requires a smaller magnetic field when  $R$  increases. Figure 3 shows the hysteresis loops of the 8-nm-thick asymmetric ring with  $R$  values of 0.1, 0.2 and 0.3. Inset of Figure 3 is a close-up of the hysteresis switching region. It shows that with  $R$  increasing, the magnetic fields needed to depin the trapped domain wall become smaller.

In ferromagnetic materials, the magnetic configurations are determined by the minimization of the sum of energy terms, i.e., the magnetostatic, the exchange, the anisotropy, and the Zeeman energies. In the permalloy thin

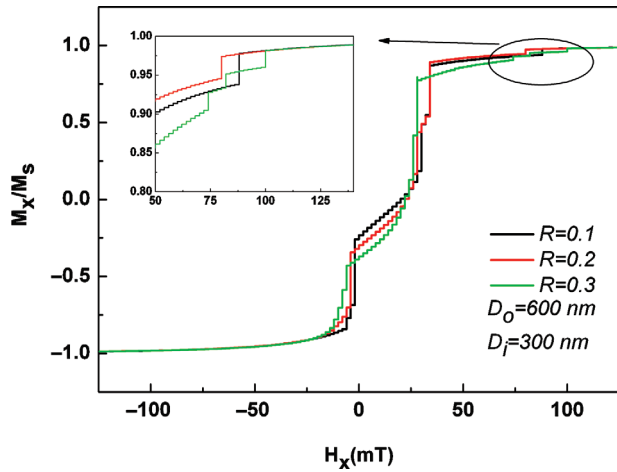


**Fig. 3.** Influence of the asymmetry on the annihilation fields. Inset shows the switch corresponding to the annihilation of the trapped domain walls. With larger asymmetry, the annihilation field for the trapped domain walls becomes smaller.

film nanoring, the magnetization is in in-plane direction because of the shape anisotropy, and the magnetic crystalline anisotropy is considered negligible. The spin configurations are determined mainly by the competition of the exchange energy and the magnetostatic energy.<sup>9</sup> To derive the exchange energy term, we use strips with finite center angle  $\Delta\theta$  to approximate a part of the asymmetric ring by segmenting the asymmetric ring into arcs of rings with different diameter. Therefore, the narrow arm of the asymmetric ring can be considered as parts of a narrow symmetric ring (I in Fig. 1) while the wide arm of the asymmetric ring can be treated as parts of a wide symmetric ring (II in Fig. 1). The exchange energy density in a ring can be calculated by considering the ring as a flux-closure spin circle with a radius  $r$ , and the distance between the neighboring spin is the atomic distance of the material  $\alpha$ . The number of magnetic moment is  $2\pi r/\alpha$ . The exchange energy of a pair of atoms is  $\Delta E = -2AS^2\cos\Phi$ , which can be approximate as  $AS^2\Phi^2$ , where  $A$  is the exchange stiffness constant of the material and  $\Phi$  is the angle between neighboring spins. We assumed  $\Phi = \alpha/r$  when the neighboring spin direction does not change abruptly. In an atomic strip arc of  $r\Delta\theta$ , the exchange energy should be  $r\Delta\theta\Delta E$ . Integrating over the asymmetric ring the exchange energy  $\varepsilon_{ex}$  is:

$$\varepsilon_{ex} = \int_0^{2\pi} \int_{R_i}^r \frac{r}{\alpha} AS^2 \left(\frac{\alpha}{r}\right)^2 dr d\theta$$

The relationship between the radius of the arc and  $\theta$  in an asymmetric ring can be expressed as

$$-2lr \cos \theta = l^2 + r^2 - R_o^2$$

For the magnetostatic energy, it has the same amplitude as the demagnetization energy which is due to the

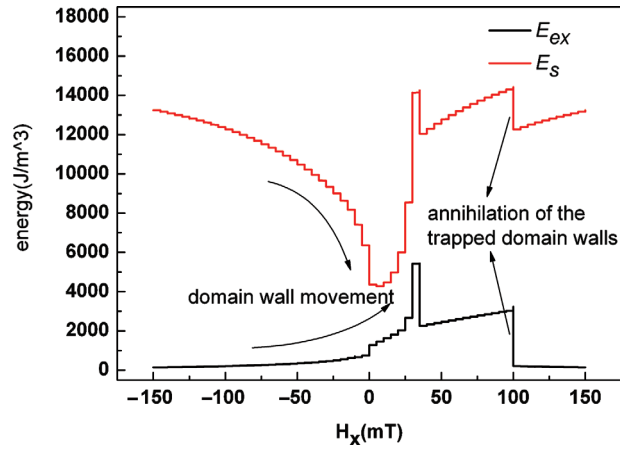


**Fig. 4.** Diagram of simulated exchange energy and magnetostatic energy during the magnetic switching.

surface charging in the thin film structures. So the magnetostatic energy can be determined by calculating the demagnetization energy. The relationship between demagnetizing factors of a ring ( $N_r$ ) and a disk ( $N_d$ )<sup>10</sup> is

$$\frac{N_r}{N_d} = \left(\frac{R_o}{R_o - R_i}\right)^{0.68}$$

Therefore, the demagnetization energy  $\Delta E_d$  in an arc with a center angle  $\theta$  can be expressed as

$$\Delta E_d = \frac{1}{2} \mu_o \left(\frac{r}{r - R_i}\right)^{0.68} N_d \cdot M_s \cdot \Delta\theta$$

where  $\mu_o$  is the material susceptibility,  $M_s$  is the saturation magnetization. The values of the demagnetizing factors for the disk with different ratios of height to diameter can be obtained from the results<sup>10</sup> reported by Chen et al. From the derived energy expression, it indicates that when the domain wall that formed at the asymmetric axis (AC) move to the narrowest point in the asymmetric ring (B), the magnetostatic energy decreases significantly. Though the domain wall movement causes the exchange energy to increase, the total energy cost is still lower than the gain. Figure 4 is the diagram of the simulated exchange energy and the magnetostatic energy during the magnetic switching. The diagram reveals that due to the domain wall movement, the drop of the demagnetization energy is much faster than the increase of the exchange energy, which is in accordance with our derivation. It therefore explains the two domain walls sliding to the narrow arm of the 8-nm-thick asymmetric ring. The annihilation of the two domain walls requires a large energy cost which corresponding to the big switches in the simulated energy loop at a field of around 100 mT. Therefore, the two domain walls reside in the narrower part of the asymmetric ring until a relatively large magnetic field is applied.

#### 4. CONCLUSIONS

In conclusion, the field-dependent switching process of permalloy asymmetric rings has been studied using micromagnetic simulations. Our simulation results show that by controlling the geometry of the magnetic nanoring, a nucleation free switching process can be obtained. During the magnetization reversal process, a pair of head-to-head and tail-to-tail domain walls is trapped at the narrow arm of the asymmetric ring. For asymmetric ring with a larger asymmetry ratio, a smaller magnetic field is needed to annihilate the trapped domain walls. The trapping behavior is found to be dependent mainly on the thickness of the asymmetric ring. Such domain wall trapping feature has potential application for magnetic memory devices.<sup>11</sup> Most importantly, our results have shown that it is possible to control the domain wall position without having to create defects or notches<sup>12</sup> in the nanoscale ring.

**Acknowledgment:** This work is supported by the ASTAR SERC grant (0821010015) and the National Research Foundation (CRP-project: Multifunctional Spintronic Materials and Devices).

#### References and Notes

1. S. S. P. Parkin, M. Hayashi, and L. Thomas, *Science* 320, 190 (2008).
2. R. P. Cowburn, D. K. Koltsov, A. O. Adeyeye, M. E. Welland, and D. M. Tricker, *Phys. Rev. Lett.* 83, 1042 (1999).
3. M. Hayashi, L. Thomas, R. Moriya, C. Rettner, and S. S. P. Parkin, *Science* 320, 209 (2008).
4. M. Klaui, C. A. F. Vaz, J. Rothman, J. A. C. Bland, W. Wernsdorfer, G. Faini, and E. Cambril, *Phys. Rev. Lett.* 90, 09720 (2003).
5. D. Petit, A. V. Jausovec, D. Read, and R. P. Cowburn, *J. Appl. Phys.* 103, 11430 (2008).
6. D. A. Allwood, G. Xiong, C. C. Faulkner, D. Atkinson, D. Petit, and R. P. Cowburn, *Science* 309, 1688 (2005).
7. J. He and S. Zhang, *Appl. Phys. Lett.* 90, 14250 (2007).
8. OOMMF simulation program is available at <http://math.nist.gov/oommf>.
9. C. A. F. Vaz, T. J. Hayward, J. Llandro, F. Schackert, D. Morecroft, J. A. C. Bland, M. Klaui, M. Laufenberg, D. Backes, U. Rudiger, F. J. Castano, C. A. Ross, L. J. Heyderman, F. Nolting, A. Locatelli, G. Faini, S. Cherifi, and W. Wernsdorfer, *J. Phys. Condens. Matt.* 19, 056501 (2007).
10. D. X. Chen, E. Pardo, and A. Sanchez, *IEEE. Trans. Magn.* 37, 3877 (2001).
11. O. Boulle, J. Kimling, P. Warnicke, M. Klaui, U. Rudiger, G. Malinowski, H. J. M. Swagten, B. Koopmans, C. Ulysse, and G. Faini, *Phys. Rev. Lett.* 101, 21660 (2008).
12. M. Klaui, *J. Phys. Condens. Matt.* 20, 31300 (2008).

Received: 7 July 2009. Accepted: 23 October 2009.

Delivered by Ingenta to: Nanyang Technological University  
IP: 155.69.24.171 On: Mon, 14 Nov 2016 09:16:08  
Copyright: American Scientific Publishers